Report

Cell Reports

Columnar-Intrinsic Cues Shape Premotor Input Specificity in Locomotor Circuits

Graphical Abstract

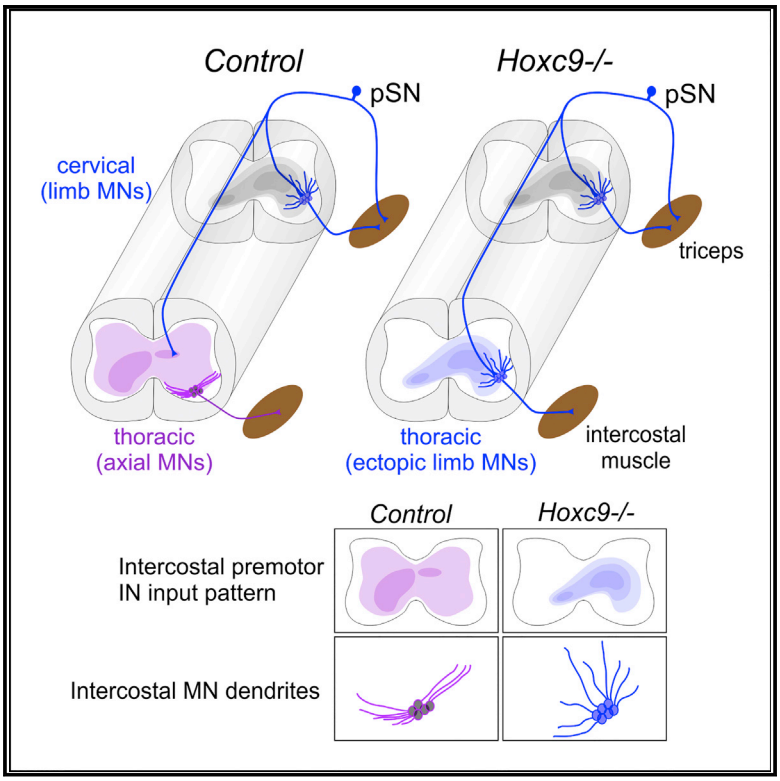

Authors

Myungin Baek, Chiara Pivetta, Jeh-Ping Liu, Silvia Arber, Jeremy S. Dasen

Correspondence

jeremy.dasen@nyumc.org

In Brief

Baek et al. show that Hox transcription-factor-dependent programs in motor neurons determine the specificity of presynaptic inputs from sensory neurons and interneurons. These findings indicate that motor neuron intrinsic programs play an instructive role in shaping the architecture of locomotor circuits.

Highlights

- MN columnar identity influences premotor input specificity in motor circuits
- Loss of *Hoxc9* disrupts sensory-motor matching in type Ia stretch reflex circuits
- Premotor interneuron input pattern is shaped by MN topographic organization
- MN-intrinsic programs contribute to locomotor circuit architecture

Baek et al., 2017, Cell Reports *21*, 867–877
October 24, 2017
https://doi.org/10.1016/j.celrep.2017.10.004

Cell Reports
Report

Columnar-Intrinsic Cues Shape Premotor Input Specificity in Locomotor Circuits

Myungin Baek,[1] Chiara Pivetta,[2,3] Jeh-Ping Liu,[4] Silvia Arber,[2,3] and Jeremy S. Dasen[1,5,*]
[1]Neuroscience Institute, Department of Neuroscience and Physiology, NYU School of Medicine, New York, NY 10016, USA
[2]Biozentrum, Department of Cell Biology, University of Basel, Klingelbergstrasse 70, 4056 Basel, Switzerland
[3]Friedrich Miescher Institute for Biomedical Research, Maulbeerstrasse 66, 4058 Basel, Switzerland
[4]Department of Neuroscience, University of Virginia School of Medicine, Charlottesville, VA 22908, USA
[5]Lead Contact
*Correspondence: jeremy.dasen@nyumc.org
https://doi.org/10.1016/j.celrep.2017.10.004

SUMMARY

Control of movement relies on the ability of circuits within the spinal cord to establish connections with specific subtypes of motor neuron (MN). Although the pattern of output from locomotor networks can be influenced by MN position and identity, whether MNs exert an instructive role in shaping synaptic specificity within the spinal cord is unclear. We show that Hox transcription-factor-dependent programs in MNs are essential in establishing the central pattern of connectivity within the ventral spinal cord. Transformation of axially projecting MNs to a limb-level lateral motor column (LMC) fate, through mutation of the *Hoxc9* gene, causes the central afferents of limb proprioceptive sensory neurons to target MNs connected to functionally inappropriate muscles. MN columnar identity also determines the pattern and distribution of inputs from multiple classes of premotor interneurons, indicating that MNs broadly influence circuit connectivity. These findings indicate that MN-intrinsic programs contribute to the initial architecture of locomotor circuits.

INTRODUCTION

Circuits within the vertebrate brainstem and spinal cord are capable of generating motor output that reflect the rhythm and pattern of muscle activation deployed during basic motor behaviors, including walking and breathing (Goulding, 2009; Grillner, 2006). The assembly of motor circuits relies on the specificity of synaptic connections established between motor neurons, proprioceptive sensory neurons, and spinal interneurons (INs) during embryonic development (Arber, 2012; Catela et al., 2015). In the networks controlling locomotion, limb muscle activation sequences are orchestrated by central pattern generators (CPGs) composed of several classes of excitatory and inhibitory spinal INs (Goulding, 2009). The activities of locomotor CPGs can be adjusted by muscle-derived sensory feedback transmitted by proprioceptive sensory neurons (pSNs), which synapse with local IN and MN subtypes (Rossignol et al., 2006). Although circuits comprising CPGs, motor neurons (MNs), and pSNs are essential for coordinating locomotor output, the mechanisms through which they assemble into functional networks are poorly understood.

A critical step in locomotor circuit assembly is the selective targeting of limb muscles by spinal MNs. A network of Hox transcription factors is required for the specification of limb-innervating lateral motor column (LMC) neurons, as well as its resident MN pools targeting individual muscles (Jessell et al., 2011; Philippidou and Dasen, 2013). While the specification of MNs by *Hox* genes is critical for muscle target specificity, the extent to which MN identity contributes to central connectivity in motor networks is unclear (Dasen, 2017). Studies investigating the assembly of spinal reflex circuits have led to differing conclusions about the relative importance of MNs. Evidence supporting an MN-independent program has emerged through the analysis of connections between pSNs and MNs under conditions where motor pool specification programs are lost. Mutation in the Hox-dependent transcription factor *Foxp1* strips LMC neurons of MN pool-specific programs, and motor axons select muscle targets in a random manner (Dasen et al., 2008; Rousso et al., 2008). Nevertheless, pSNs project to the appropriate dorsoventral position within the ventral spinal cord and synapse with MNs, regardless of which limb muscle is targeted (Sürmeli et al., 2011).

In contrast, analyses of sensory-motor connectivity under conditions where only a subset of MN pools are affected provide evidence that target-induced molecular recognition programs can direct specificity in reflex circuits. Expression of the transcription factor *Pea3* is induced by limb-derived neurotrophins in MNs, and in the absence of *Pea3*, pSNs target inappropriate MN subtypes (Livet et al., 2002; Vrieseling and Arber, 2006). Pea3 controls expression of the guidance receptor ligand *Sema3e*, and while MN position is unaffected in *Sema3e* mutants, pSNs target inappropriate MNs (Pecho-Vrieseling et al., 2009). Although target-induced expression of guidance determinants is one strategy for controlling specificity in reflex circuits, they appear to operate in only a limited number of MN pools. Given that Hox proteins govern MN diversification independent of peripheral signals (Dasen et al., 2005), key aspects of sensory-motor connectivity could be controlled through MN-intrinsic pathways.

Beyond spinal reflex circuits, evidence suggests that MNs may play broader roles in determining connectivity with multiple neuronal populations, including the diverse classes of premotor INs that constitute CPG networks. Although loss of an LMC

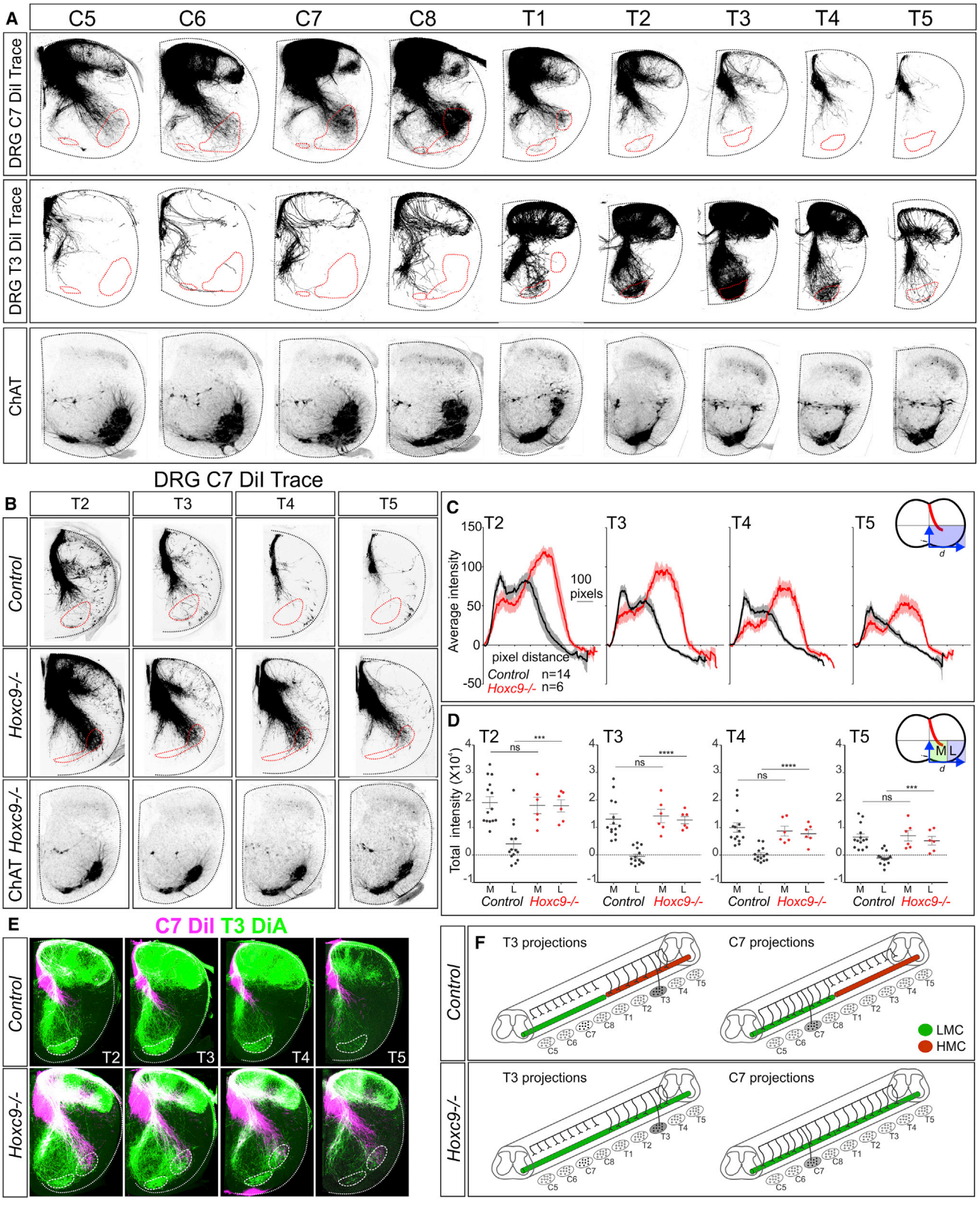

(legend on next page)

identity in *Foxp1* mutants has no apparent effect on the central targeting of pSN axons, the pattern of output from locomotor CPGs is disrupted. In *Foxp1* mutants, there is a loss of extensor-like bursting pattern, suggesting that molecular programs acting within LMC neurons contribute to connectivity between spinal INs and specific MN subtypes (Hinckley et al., 2015; Machado et al., 2015). In addition, MN columns targeting limb and axial muscle have been shown to be engaged by distinct populations of premotor INs (Goetz et al., 2015). While these studies suggest that MNs contribute to locomotor network activity, it has not been investigated whether MNs influence connectivity with spinal INs.

In this study, we assessed whether MN identity and organization determine the specificity of inputs from premotor neurons. We show that transformation of MNs targeting hypaxial muscle to a limb-level LMC fate causes marked changes in the central projections and target specificity of proprioceptive sensory neurons. Conversion of axial MNs to an LMC fate also alters the distribution of inputs from spinal premotor INs, indicating a prominent role for MNs in motor circuit assembly.

RESULTS

Hoxc9 Activity Shapes the Central Pattern of Cervical Sensory Neuron Projections

To determine whether MN identity contributes to the specificity of connections within the ventral spinal cord, we examined the formation of sensory-motor reflex circuits under conditions where MN organization has been genetically altered. We first traced the central projections of sensory neuron (SN) afferents along the rostrocaudal axis in controls by injecting the lipophilic dye DiI into the dorsal root ganglia (DRGs) of postnatal day (P)0–P1 mice. Cervical (C) DRGs contain pSNs targeting predominantly forelimb muscles, whereas thoracic (T) pSNs target dorsal epaxial and ventral hypaxial muscles. This analysis revealed that the projections of cervical and thoracic SNs to MNs were restricted to segments where the corresponding columnar subtypes are present, whereas central branches at other segmental levels terminate in the intermediate spinal cord. Anterograde tracing from DRG C7 labeled sensory afferents projecting to the ventral spinal cord between segments C5 and T1, where the cell bodies of LMC neurons reside (Figure 1A). In contrast, at thoracic segments (T2–T5), cervical SN collaterals terminated in the intermediate spinal cord (Figure 1A). Similarly, tracing from thoracic DRGs labeled sensory neurons projecting to thoracic MNs but were restricted to the intermediate spinal cord at cervical levels (Figure 1A). These data indicate that the central afferents of cervical SNs target LMC neurons, while thoracic SNs target MNs in thoracic segments.

To explore whether MN identity influences the central projection of SNs, we traced afferents under conditions where the columnar fate of MNs has been transformed. The *Hoxc9* gene is expressed at thoracic levels and is essential for the organization of MN subtypes along the rostrocaudal axis. In *Hoxc9* mutants, thoracic hypaxial motor column (HMC) and preganglionic motor column (PGC) neurons are converted to an LMC fate, in part, due to the derepression of cervical *Hox4–Hox8* genes and *Foxp1* at thoracic levels (Jung et al., 2010). To determine whether the ventral termination zones of SN afferents are influenced by MN columnar identity, we examined sensory projections in global *Hoxc9* mutants. Injection of DiI into DRG C7 in *Hoxc9* mutants labeled sensory axons extending to the ventrolateral thoracic spinal cord, where ectopic LMC neurons reside (Figure 1B). Sensory neurons originating from C7 targeted the ventrolateral spinal cord over multiple segments in *Hoxc9* mutants, extending from T2 to T5 (Figures 1B–1D). Injection of DiI into DRGs C5, C6, and C8 in *Hoxc9* mutants also labeled sensory afferents extending to MNs at thoracic levels, revealing that the loss of *Hoxc9* has a widespread effect on the central targeting of forelimb-level sensory neurons (Figure S1A).

In principle, the extension of limb SNs to thoracic MNs could compete with the ability of thoracic SNs to target MNs. We, therefore, assessed the consequences of the presence of limb sensory axons on the projection of thoracic sensory afferents to MNs. Thoracic SNs were traced by DiA injection into DRG T3, while cervical sensory afferents were traced in parallel by the injection of DiI into DRG C7. This analysis revealed that both cervical and thoracic SNs project afferents into the region occupied by ectopic LMC neurons (Figure 1E). These results indicate that, in the absence of *Hoxc9*, limb-level SNs extend axons toward ectopic LMC neurons but do not preclude the ability of thoracic SNs to target the ventral spinal cord (Figure 1F).

Supernumerary axonal projections are often generated during the early stages of neuronal development and are subsequently removed as circuits mature (Luo and O'Leary, 2005). The extension of limb SNs to thoracic MNs in *Hoxc9* mutants might reflect the maintenance of projections that existed at earlier stages. We, therefore, assessed whether limb SNs initially project collaterals to thoracic MNs. DiI was injected into DRG C8 between embryonic day (E)12.5 and E18.5, and the central projections of SNs

Figure 1. Hox-Dependent Programs Establish the Central Pattern of Sensory Projections

(A) Projections of SNs along the rostrocaudal axis of the spinal cord in control animals at P1. SNs were traced by DiI injection into DRG C7 and T3, and central projections were analyzed at indicated segments. Projections include a medial branch directed toward median motor column (MMC) neurons and a lateral branch to non-MMC populations (LMC and HMC neurons). Bottom panels show choline acetyltransferase (ChAT) expression in MNs between segments C5 and T5.

(B) Projection of SNs to MNs in thoracic segments after DiI injections into DRG C7 in control and *Hoxc9*$^{-/-}$ mice at P0. Approximate MN position is outlined in red, based on ChAT.

(C) Quantification of DiI pixel intensity along the mediolateral axis in control and *Hoxc9*$^{-/-}$ mice. Lines show mean pixel intensity ± SEM from 14 controls (E18.5, n = 7; P0, n = 7) and 6 *Hoxc9*$^{-/-}$ mice (E18.5, n = 4; P0, n = 2). Inset shows region where distance (d) and pixel intensity (i) were measured.

(D) Quantification of total DiI pixel intensity in medial and lateral regions of the spinal cord. In *Hoxc9* mutants, there is an increase in lateral projections. For T2, ***p = 0.0007. For T3, ****p < 0.0001. For T4, ****p < 0.0001. For T5, ***p = 0.0003.

(E) Comparison of C7 (DiI) and T3 (DiA) SN projections. Both C7 and T3 SNs project to MNs in *Hoxc9*$^{-/-}$ mice.

(F) Summary of SN projections from T3 and C7 in control and *Hoxc9*$^{-/-}$ mice.

See also Figure S1.

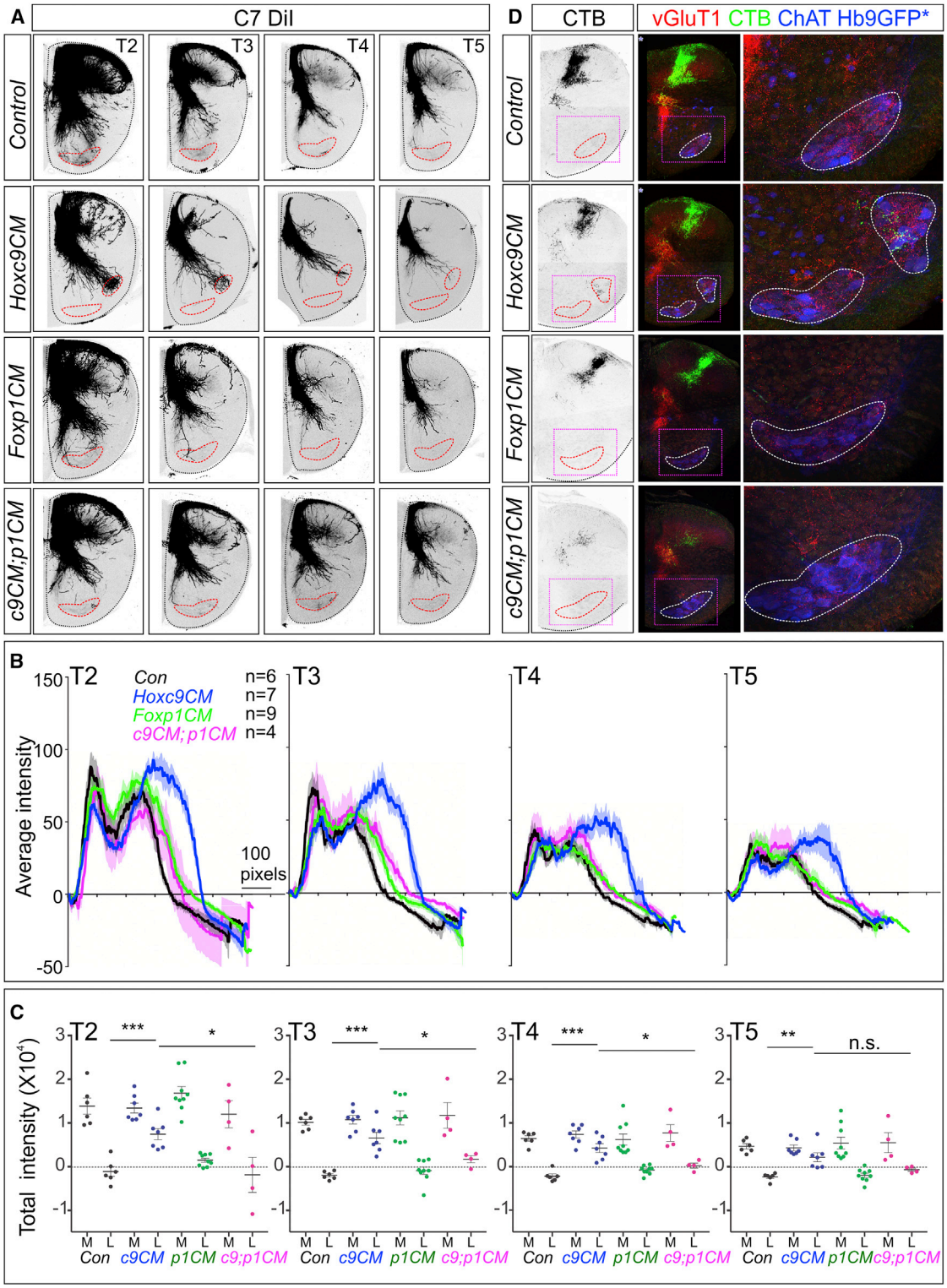

Figure 2. MN Columnar Identity Shapes Sensory-Motor Connectivity

(A) DiI tracing from DRG C7 analyzed at thoracic segments T2–T5 in indicated mouse mutants at P0. In *Hoxc9*^{CM}; *Foxp1*^{CM} double mutants and *Foxp1*^{CM} mice, SNs do not project to thoracic MNs.

(B) Quantification of DiI-traced DRG C7 sensory afferents in the ventrolateral quadrant of segments T2–T5. Number of animals analyzed: control, n = 6 (P0, n = 6); *Hoxc9*^{CM}, n = 7 (P0, n = 7); *Foxp1*^{CM}, n = 9 (E18.5, n = 3; P0, n = 6); *Hoxc9*^{CM}; *Foxp1*^{CM}, n = 4 (P0, n = 4).

(legend continued on next page)

were analyzed in cervical and thoracic segments. In control mice, SNs originating from C8 enter the spinal cord by E13.5, approach the ventral spinal cord at E14.5, and target cervical MNs by E15.5 (Figure S1B). Although cervical sensory afferents extend to thoracic segments, they did not project to thoracic MNs at any stage in control animals. In *Hoxc9* mutants, C8-derived SNs extend to thoracic MNs over the same time window as cervical LMC neurons, beginning at E15.5 (Figure S1B). The projection of limb SNs to thoracic MNs in *Hoxc9* mutants, therefore, does not result from the maintenance of projections that existed earlier.

The *Hoxc9* gene is expressed by INs and non-neuronal tissues, raising the question of whether the observed phenotypes are specifically due to the transformation of MN columnar identities. To address this, we selectively removed *Hoxc9* from the ventral spinal cord. We generated a floxed *Hoxc9* allele and crossed this line with *Olig2::Cre* mice, in which Cre is expressed by MN progenitors, and transiently by V2 and V3 IN precursors (Chen et al., 2011; Dessaud et al., 2007) (Figures S2A–S2C). In *Hoxc9* conditional mutants (*Hoxc9*^{CM} mice), *Hoxc9* is extinguished from MNs, and *Hox* genes normally restricted to cervical levels are derepressed in thoracic MNs, similar to global *Hoxc9* mutants (Figures S2D and S2E) (Jung et al., 2010). In addition, thoracic MN columnar subtypes (PGC and HMC neurons) were depleted in *Hoxc9*^{CM} mice, and LMC neurons (defined by Foxp1 and Raldh2 expression) were ectopically generated in segments T1–T5 (Figures S2F and S2G). Ectopic LMC neurons also expressed the transcription factors Pea3 and Scip, markers for MN pools residing in caudal cervical segments (Figures S2E and S2G).

We traced sensory afferent projections from cervical DRG in *Hoxc9*^{CM} mice by DiI injection into DRG C7. Similar to *Hoxc9* global mutants, cervical SNs projected afferents into the ventral thoracic spinal cord in *Hoxc9*^{CM} mice (Figure 2A). As with global *Hoxc9* mutants, C7-derived sensory projections were directed to the lateral region of the ventral spinal cord, where ectopic LMC neurons reside (Figures 2B and 2C). These observations indicate that the changes in sensory projections in *Hoxc9* mutants are specifically due to neuronal transformations in the ventral spinal cord.

Limb pSNs Establish Functional Synapses with Ectopic LMC Neurons in *Hoxc9* Mutants

Tracer injection into DRGs indiscriminately labels multiple classes of SNs, raising the questions of whether the ectopic projections in *Hoxc9* mutants derive from proprioceptive SNs and whether they establish functional connections with MNs. We used muscle-specific tracer injections to assess whether synapses are established between limb pSNs and thoracic LMC neurons in *Hoxc9* mutants. Forelimb pSNs were traced by injection of cholera toxin subunit B (CTB) into the triceps muscle at P3, and synapses with MNs were examined at P5. Boutons on MNs were visualized through colocalization of CTB with vesicular glutamate transporter 1 (vGluT1), which labels the terminals of type Ia pSN afferents. In control mice, vGluT1^{+}; CTB^{+} terminals of triceps pSNs localized to the dorsomedial thoracic spinal cord, similar to the restriction observed in DiI tracing (Figures 3A and 3E). In contrast, in global and conditional *Hoxc9* mutants, vGluT1^{+}; CTB^{+} triceps pSN terminals localized to the ventrolateral thoracic spinal cord where ectopic LMC MNs are located (Figures 3A and 3E). In global *Hoxc9* mutants, vGluT1^{+}; CTB^{+} terminals of triceps pSNs were observed on the soma of thoracic MNs but were not observed in control animals (225.9 ± 54.44 [mean ± SEM] synapses per 30-μm section in [n = 5] *Hoxc9*$^{-/-}$ mice versus 0 ± 0 in [n = 5] control mice; **p = 0.0032) (Figures 3B and 3C). Similarly, tracing from the triceps muscle in *Hoxc9*^{CM} mice labeled vGluT1^{+} terminals that extended ventrally and established synapses with MNs (45.48 ± 11.09 [mean ± SEM] synapses per 30-μm section in [n = 8] *Hoxc9*^{CM} mice versus 0 ± 0 in [n = 6] controls; **p = 0.0043) (Figures 3F and 3G). Ectopic synapses on thoracic MNs were also observed after tracer injections into biceps, distal flexor, and distal extensor limb muscles in *Hoxc9*^{CM} mice (Figure S3A). These results indicate that limb pSNs establish synapses with ectopic LMC neurons in *Hoxc9* mutants.

Because the observed connections between limb pSNs and ectopic LMC neurons could be attributed to a rerouting of thoracic MNs to limb muscle, we assessed the position of the triceps MN pool, as well as the peripheral target specificity of supernumerary LMC neurons in *Hoxc9* mutants. Retrograde tracing from triceps in *Hoxc9*$^{-/-}$ and *Hoxc9* ^{CM} mice labeled MNs restricted to segments C5–T1, similar to controls (Figure S3B), indicating that ectopic LMC neurons are not rerouted to the limb. Because ectopic LMC neurons have been shown to target intercostal muscle in *Hoxc9* mutants (Jung et al., 2010), we assessed triceps pSN-thoracic LMC connectivity after the injection of tracers into each of these muscle groups. This analysis revealed that thoracic LMC neurons target intercostal muscles and receive input from triceps pSNs (Figure S3C). In addition, the distribution of cervical SNs targeting triceps muscle was unaffected in *Hoxc9* mutants (Figure S3D), indicating that the alterations in sensory-motor connectivity are not due to changes in the source of pSNs targeting the triceps.

We next assessed whether limb pSNs have the capacity to deliver sensory information to ectopic LMC neurons in *Hoxc9* mutants. We isolated spinal cords from *Hoxc9* mutants, stimulated C7 dorsal roots, and measured MN responses by ventral root recordings at segmental levels C7 and T3 (Figure S3E). In both control and *Hoxc9* mutants, after C7 dorsal root stimulation, C7 MNs exhibited short-latency monosynaptic responses,

(C) Quantification of total DiI pixel intensity in medial and lateral regions of the spinal cord. Pixel intensities in the lateral position in *Hoxc9*^{CM}; *Foxp1*^{CM} and *Foxp1*^{CM} mice are similar to those in controls. For T2: *p = 0.0219; ***p = 0.0004. For T3: *p = 0.0274; ***p = 0.0001. For T4: *p = 0.0192; ***p = 0.0002. For T5: **p = 0.0025; ns = 0.0747.

(D) Analysis of triceps sensory terminals in segment T3 at P5. In *Hoxc9*^{CM}; *Foxp1*^{CM} mice, no CTB^{+} terminals are observed in the ventral spinal cord. n = 3 for each genotype.

Images are composites of tiles created in Zen software (Zeiss).

See also Figure S2.

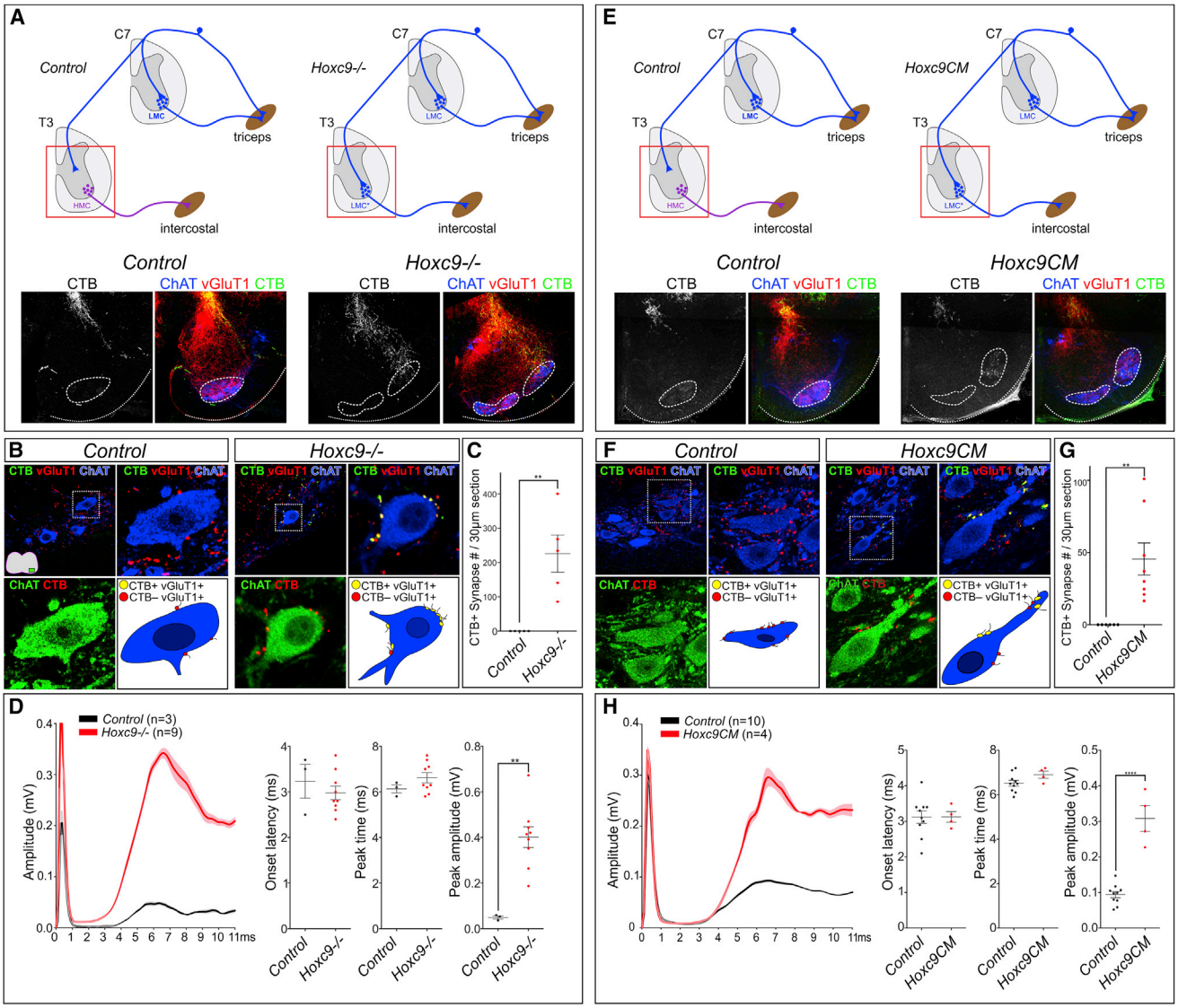

Figure 3. Limb pSNs Establish Synapses with Ectopic LMC Neurons in *Hoxc9* Mutants

(A) Localization of triceps pSN terminals in control and *Hoxc9*$^{-/-}$ mice at thoracic levels. Cervical pSN terminals were traced by injection of CTB into triceps muscles at P3 and examined at P5 at segment T3.

(B) Triceps pSN terminals establish synapses on thoracic MNs in *Hoxc9*$^{-/-}$ mice. CTB^{+};vGluT1^{+} terminals are observed on MNs, marked by ChAT.

(C) Quantification of CTB^{+} terminals on MNs at segment T3. Total synapses were counted in 30-µm sections. Controls: n = 5, 0 ± 0 (mean ± SEM); *Hoxc9*$^{-/-}$ mice: n = 5, 225.9 ± 54.44; **p = 0.0032.

(D) Traces of T3 ventral root signals upon C7 dorsal root stimulation in control and *Hoxc9*$^{-/-}$ mice at P6. Quantification of onset latencies (control, 3.23 ± 0.37 ms; *Hoxc9*$^{-/-}$, 2.99 ± 0.15 ms), peak times (control, 6.13 ± 0.18 ms; *Hoxc9*$^{-/-}$, 6.62 ± 0.22 ms), and peak amplitudes (control, 0.05 ± 0.01 mV; *Hoxc9*$^{-/-}$, 0.40 ± 0.05 mV; **p = 0.0015). Bars on graphs indicate mean ± SEM.

(E) CTB tracing of triceps sensory terminals in thoracic segments of control and *Hoxc9*^{CM} mice.

(F) Images of CTB-traced triceps pSNs in thoracic segments. In *Hoxc9*^{CM} mice, CTB^{+};vGluT1^{+} terminals were observed on MNs.

(G) Quantification of CTB^{+};vGluT1^{+} terminals on thoracic MNs in control and *Hoxc9*^{CM} mice. Controls: n = 6, 0 ± 0 (mean ± SEM); *Hoxc9*^{CM}: n = 8, 45.48 ± 11.09. Bars indicate mean ± SEM; **p = 0.0043.

(H) Traces of T3 ventral root signals upon C7 dorsal root stimulation in control (n = 10) and *Hoxc9*^{CM} mice (n = 4) at P6. Lines indicate mean ± SEM. Quantification of onset latencies (control, 3.12 ± 0.17; *Hoxc9*^{CM}, 3.13 ± 0.153), peak times (control, 6.52 ± 0.13; *Hoxc9*^{CM}, 6.90 ± 0.16), and peak amplitudes (control, 0.1 ± 0.01; *Hoxc9*^{CM}, 0.31 ± 0.04; ****p < 0.0001). Bars indicate mean ± SEM.

Images are composites of tiles created in Zen software (Zeiss).

See also Figure S3.

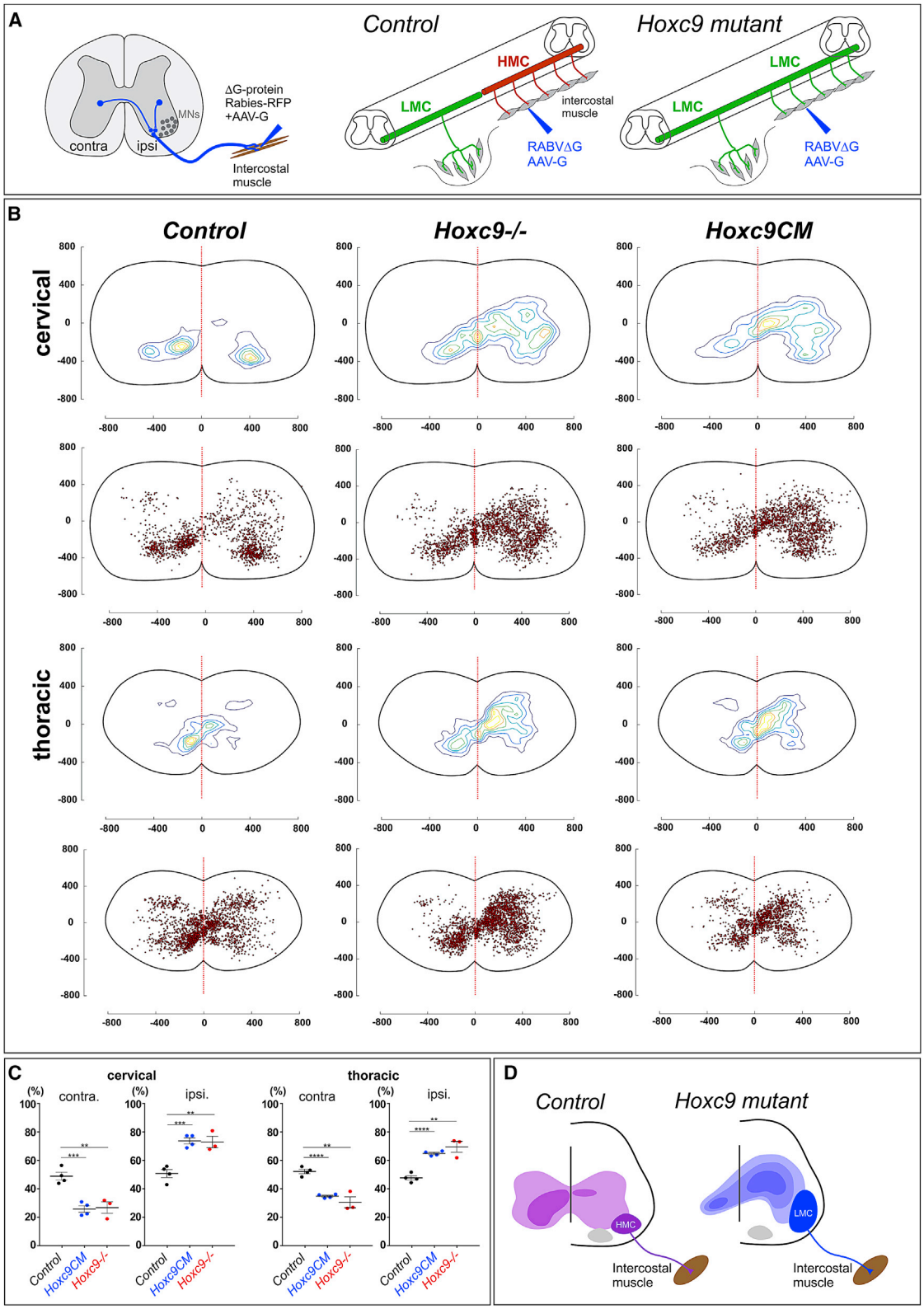

(legend on next page)

followed by slower polysynaptic responses (Figure S3E). Onset latencies, monosynaptic response peak times, and peak amplitudes were not significantly different between control and *Hoxc9* mutants at C7 (Figure S3E). In contrast, in global *Hoxc9* mutants, T3 ventral roots showed responses that were markedly increased in amplitude (0.40 ± 0.05 mV in [n = 9] $Hoxc9^{-/-}$ mice versus 0.05 ± 0.01 mV in [n = 3] controls; **p = 0.0015) (Figure 3D). Similarly, in $Hoxc9^{CM}$ mice, upon C7 dorsal root stimulation, response amplitudes at T3 were markedly increased (0.31 ± 0.04 mV in [n = 4] $Hoxc9^{CM}$ mice versus 0.1 ± 0.01 mV in [n = 10] controls; ****p < 0.0001) (Figure 3H). The increased T3 amplitudes in *Hoxc9* mutants likely reflect the presence of ectopic synapses from limb pSNs but may also be due to changes in MN input resistance, as a consequence of their transformation to an LMC fate. Onset latencies at T3 were similar between control and *Hoxc9* mutants (Figures 3D and 3H), possibly due to the presence of some sensory projections to the thoracic MNs in controls. Collectively, these data indicate that cervical pSNs establish functional connections with ectopic LMC neurons in *Hoxc9* mutants.

In *Hoxc9* mutants, the switch of MNs to an LMC fate is accompanied by a derepression of cervical *Hox* genes in both MNs and IN populations (Figure S2E). The alterations in pSN afferent connectivity could be solely due to changes in MNs, independent of changes in INs, or dependent on programs acting within both populations. To address this, we assessed whether the changes in sensory-motor connectivity in *Hoxc9* mutants rely on the LMC determinant *Foxp1*, a transcription factor essential for LMC specification (Dasen et al., 2008; Rousso et al., 2008). To remove both *Hoxc9* and *Foxp1* from MNs, we combined *Hoxc9 flox*, *Foxp1 flox*, and *Olig2::Cre* alleles. In $Hoxc9^{CM}$; $Foxp1^{CM}$ mice, no ectopic Raldh2^{+} MNs were detected at thoracic levels (Figure S2F). In contrast, a *Hox* gene normally expressed at cervical levels, *Hoxc6*, was derepressed in the thoracic MNs of both $Hoxc9^{CM}$;$Foxp1^{CM}$ and $Hoxc9^{CM}$ mice (Figure S2E). Combined removal of *Foxp1* and *Hoxc9* in MNs, therefore, prevents the generation of ectopic LMC neurons but still leads to the derepression of cervical *Hox* genes (Figure S2G).

Cervical sensory afferents were traced by DiI injection into DRG C7 of $Hoxc9^{CM}$;$Foxp1^{CM}$ mice. Ventrally extending sensory afferents were not observed at thoracic levels after the combined removal of *Hoxc9* and *Foxp1* (Figures 2A–2C). Limb pSN afferents were also traced by CTB injection into the triceps muscle in double conditional mutants. No vGluT1^{+};CTB^{+} terminals were observed on thoracic MNs (Figure 2D). In addition, the amplitudes of T3 ventral root recording after C7 dorsal root stimulation were similar between control, $Foxp1^{CM}$, and $Hoxc9^{CM}$; $Foxp1^{CM}$ mice (Figure S3F). These results indicate that the altered sensory-motor connectivity observed in *Hoxc9* mutants is due to the activation of LMC programs within thoracic MNs.

MN Columnar Organization Determines Premotor IN Input Pattern

Mutation in cell-fate determinants can affect multiple features of MNs, including neuronal settling position and dendritic architecture (Sürmeli et al., 2011; Vrieseling and Arber, 2006). In *Hoxc9* mutants, we found that transformed thoracic MNs were shifted to a more dorsolateral position, and their dendrites project radially, similar to cervical LMC neurons (Figures S4A–S4C). These changes in somatodendritic architecture could, in principle, affect MN connectivity with several premotor populations, including the diverse classes of spinal INs essential to coordinate MN firing.

Studies investigating the sources of spinal INs targeting MNs have revealed marked differences in the types and distribution of INs that synapse with specific columnar subtypes (Goetz et al., 2015). LMC neurons receive inputs from premotor INs that are positioned predominantly ipsilateral to the target limb. In contrast, thoracic HMC neurons receive inputs from INs that are distributed both contralaterally and ipsilaterally, with bias toward contralateral populations. To determine whether MN columnar identity has a role in shaping IN connectivity patterns, we examined premotor inputs in *Hoxc9* mutants. Because ectopic LMC neurons project to the normal muscle targets of thoracic HMC neurons (Jung et al., 2010), we assessed premotor INs that synapse with MNs targeting intercostal muscle.

Premotor INs were labeled via viral monosynaptic tracing methods (Stepien et al., 2010; Tripodi et al., 2011). Glycoprotein-deficient rabies virus expressing RFP protein (Rab-RFP) and adeno-associated virus expressing glycoprotein (AAV-G) were injected intramuscularly (Figure 4A). Viruses were injected into rostral intercostal muscles at P5, and the distribution of labeled premotor IN populations was examined at cervical and thoracic levels at P13. In controls, intercostal premotor INs were evenly distributed between the ipsilateral and contralateral sides of injection (48% ipsilateral versus 52% contralateral at thoracic levels) (Figures 4B and 4C). In contrast, in global *Hoxc9* mutants, premotor INs were shifted toward an ipsilateral bias (70% ipsilateral versus 30% contralateral at thoracic levels) (Figures 4B and 4C), a distribution similar to that of LMC premotor IN populations (Goetz et al., 2015). The ipsilateral shift in the

Figure 4. MN Columnar Identity Determines Premotor IN Input Pattern

(A) Schematic of viral tracing strategy. AAV-G and RABVΔG-RFP viruses were co-injected into rostral intercostal muscles at P5 and examined at P13.

(B) Contour plots representing labeled premotor INs position. The regions with the greatest labeling density are encircled with a yellow line. A red dotted line indicates the midline of the spinal cord. Distances (in micrometers) from the central canal are shown on the x and y axes. Cervical regions (C1–C8) and thoracic regions (T1–T13) are shown separately. Labeled cell position is shown beneath contour plots. Total number of labeled neurons in control mice: n = 4 mice; 1,385 cells (cervical); 1,895 cells (thoracic). Total number of labeled neurons in $Hoxc9^{CM}$ mice: n = 4 mice; 1,823 cells (cervical); 1,412 cells (thoracic). Total number of labeled neurons in $Hoxc9^{-/-}$ mice: n = 3 mice; 2,053 cells (cervical); 2,325 cells (thoracic).

(C) Quantification of ipsilateral versus contralateral premotor populations at cervical and thoracic levels. Numbers represent averages from controls (n = 4), $Hoxc9^{CM}$ mice (n = 4), and $Hoxc9^{-/-}$ mice (n = 3). **p < 0.001; ***p = 0.0001; ****p < 0.0001. Bar graphs indicate mean ± SEM.

(D) Summary of changes in premotor labeling in *Hoxc9* mutant mice.

See also Figure S4.

distribution of labeled INs was observed at both thoracic and cervical levels, reflecting changes in the connectivity of both intrasegmental and descending premotor INs.

To determine whether the shift in premotor input distribution is specifically due to changes in MNs, we performed rabies tracing experiments in *Hoxc9*^{CM} mice. As with *Hoxc9* global mutants, after tracing from intercostal muscle, there was a pronounced shift in premotor IN inputs to the ipsilateral side of the spinal cord (65% ipsilateral versus 35% contralateral at thoracic levels) (Figures 4B and 4C). Interestingly at thoracic levels, there was a loss of a population of contralateral premotor INs in *Hoxc9* global mutants that were retained in *Hoxc9*^{CM} mice (Figure 4B), suggesting that *Hoxc9* is also required in certain IN types for connectivity to MNs. These results indicate that the columnar identity of MNs has a profound impact on determining the pattern of inputs from premotor IN populations (Figure 4D).

DISCUSSION

Coordinate control of limb muscles depends on the specificity of connections established between MN subtypes and diverse classes of premotor neurons. While studies have shown that MNs can play an instructive role in defining functional properties of locomotor networks, the role of MN identity in spinal circuit assembly has remained unclear. We found that Hox-dependent programs in MNs are essential in shaping the patterns of connectivity between proprioceptive sensory neurons, spinal INs, and MN columnar subtypes. These findings indicate that MN identity plays a significant role in regulating premotor synaptic specificity in locomotor circuits.

During sensory-motor circuit assembly, proprioceptive sensory neurons synapse with MNs innervating the same muscle peripherally but avoid MNs projecting to functionally antagonistic muscles (Eccles et al., 1957; Frank and Mendelson, 1990). Studies on the mechanisms contributing to specificity in stretch-reflex circuits have largely focused on how pSNs select MN pools within a single segment (Mendelsohn et al., 2015; Sürmeli et al., 2011; Vrieseling and Arber, 2006). However, in order to achieve correct wiring, pSNs must project over multiple segments to locate the position of their appropriate postsynaptic targets. Remarkably, a single pSN can establish highly selective connections with each of the ~50–200 MNs within a pool supplying a given limb muscle (Mendell and Henneman, 1968). Although sensory neurons are known to project long distances along the rostrocaudal axis and extend ventrally to the position of MNs (Eide and Glover, 1995; Ozaki and Snider, 1997), the mechanisms through which they select postsynaptic targets over multiple segments are unknown.

We found that MN topographic organization determines the central termination of pSN axons within the ventral spinal cord. Transformation of thoracic HMC neurons to an LMC fate, through mutation of the *Hoxc9* gene, causes limb pSNs to extend to MNs at thoracic levels, where they establish functional connections with MNs. This alteration in connectivity does not appear to be a consequence of changes in MNs due to limb-derived signals, since ectopic LMC neurons in *Hoxc9* mutants project to hypaxial muscle. Analysis of a single muscle target in *Hoxc9* mutants revealed that limb pSNs synapse and establish functional connections with thoracic LMC neurons. These results indicate that altered central connectivity of pSNs in *Hoxc9* mutants is due to changes in MN-intrinsic programs.

In addition to establishing connections with limb pSNs, LMC neurons synapse with multiple classes of spinal INs. Recent studies have shown that MNs can exert instructive roles in determining basic properties of locomotor circuits (Hinckley et al., 2015; Machado et al., 2015; Song et al., 2016), but whether MN identity determines connectivity with spinal INs has not been tested. We found that, after global or conditional removal of *Hoxc9*, the distribution of intercostal premotor INs shifts to an ipsilateral bias, similar to patterns normally observed for limb MNs (Goetz et al., 2015). As with the alterations in sensory-motor connectivity in *Hoxc9* mutants, these changes do not appear to be due to peripheral signals provided by the limb, indicating that MN-intrinsic programs regulate connectivity between spinal INs and columnar subtypes.

Several lines of evidence indicate that the changes in central connectivity observed in *Hoxc9* mutants are specifically due to transformation of MN columnar identities. We found that the rerouting of limb pSNs to ectopic LMC neurons in *Hoxc9*^{CM} mice requires the LMC determinant *Foxp1*. After the combined removal of both *Hoxc9* and *Foxp1* from MNs, cervical sensory afferents fail to synapse with thoracic MNs, similar to controls. Although we are unable to assess premotor IN connectivity in *Hoxc9* ^{CM}*; Foxp1* ^{CM} mice, due to the lethality of this mutation, the majority of ipsilateral LMC premotor INs derive from an Lbx1^{+} domain that is not targeted by *Olig2::Cre* excision. Since our rabies tracing strategy labels INs that are connected to MNs via a single synapse, the changes in premotor input distribution reflect the loss of *Hoxc9* from MNs.

How might Hox-dependent programs in MNs determine patterns of premotor connectivity? Given the diverse roles of Hox proteins in motor axon target selectivity, the central connectivity changes observed in *Hoxc9* mutants likely involve alterations in multiple downstream molecular pathways. In addition, we found that *Hoxc9* mutation alters the settling position and dendritic architecture of transformed MN populations. The alteration in premotor connectivity in *Hoxc9* mutants, therefore, could reflect changes in both the molecular and somatodendritic features of MNs. These results are consistent with the view that sensory-motor circuit assembly relies on both positional and molecular recognition cues (Jessell et al., 2011) and extend the influence of MN subtype identity to additional premotor neuronal classes.

Locomotion requires the coordinated activation of dozens of limb muscles, which requires more selective connections between MNs and premotor populations. While our study focuses on a single *Hox* gene and the role of columnar identity in spinal circuit connectivity, a similar logic could apply to pools of MNs targeting specific limb muscles. In addition, the same *Hox* genes expressed by LMC neurons are also present in INs and pSNs, suggesting that a common group of regulatory factors drives connectivity. The assembly of locomotor circuits may depend on a set of initial cues from MN columnar subtypes that provide a broad set of instructions to premotor populations, operating in parallel with Hox-dependent programs in several neuronal classes.

EXPERIMENTAL PROCEDURES

Mouse Genetics

Animal work was approved by the Institutional Animal Care and Use Committee of the NYU School of Medicine (Protocol 160308) in accordance with NIH guidelines. Generation of floxed-*Hoxc9* mice and additional strains is described in the Supplemental Experimental Procedures. No phenotypic differences between animals of different genders are expected but were not formally tested.

DiI Tracing

Animals were perfused with PBS and 4% paraformaldehyde (PFA) and were post-fixed for 2 hr at 4°C. ~3 μL DiI-ethanol solutions were applied to a slide glass to form a thin layer of DiI crystals. DiI crystals were injected into DRGs using a sharp tungsten needle. Injected tissue was incubated in 4% PFA for 10 to ~30 days at 37°C. Spinal cords were vibratome sectioned at a thickness of 150 μm.

CTB Tracing

1%–~2% CTB (Sigma-Aldrich) solutions were injected into the triceps muscle at P3–P4 and examined after 2 days. Pups were perfused with PBS and 4% PFA. Spinal cords were isolated and post-fixed for 2–6 hr at 4°C. Tissue was vibratome sectioned (at 100 μm) or cryosectioned (at 30 μm).

Extracellular Recordings

Methods for ventral root recordings are described in the Supplemental Experimental Procedures.

Viral Tracing

Methods for viral tracing are described in the Supplemental Experimental Procedures.

Immunohistochemistry

Primary antibodies against Hox proteins, Foxp1, Isl1/2, and Raldh2 have been described previously (Dasen et al., 2005, 2008; Jung et al., 2010). Commercial antibodies included: nNos1 (rabbit, 1:10,000, Immunostar), choline acetyltransferase (ChAT) (goat, 1:200, Millipore), CTB (goat, 1:4,000, List Biological Laboratories; rabbit, 1:2000, Sigma-Aldrich), and vGluT1 (guinea pig, 1:1,000, Millipore). Detailed protocols for histology are available on the J.S.D. lab website (http://www.med.nyu.edu/dasenlab/)

Imaging and Image Processing

A Zeiss confocal microscope (LSM 700 with 20× dry or 63× oil objective lens) was used to acquire images. Images were processed in Fiji and Photoshop.

Statistics

Data were analyzed using GraphPad Prism6 software. Data are shown as averages ± SEM. Values were compared using Student's two-tailed t test, and p values less than 0.05 were considered significant. Animal numbers are indicated in the figures and legends.

SUPPLEMENTAL INFORMATION

Supplemental Information includes Supplemental Experimental Procedures and four figures and can be found with this article online at https://doi.org/10.1016/j.celrep.2017.10.004.

AUTHOR CONTRIBUTIONS

M.B. and J.S.D. devised the project, designed the experiments, and wrote the paper. C.P. and S.A. provided viral reagents and analyzed transsynaptic tracing. J.-P.L. generated the *Hoxc9* conditional allele and performed preliminary analysis of mutants. All authors read the paper.

ACKNOWLEDGMENTS

We thank Helen Kim and David Lee for technical support; Anders Enjin, Michael Long, and George Mentis for advice with electrophysiology; and Polyxeni Philippidou and Richard Mann for feedback on the manuscript. This work was supported by NIH NINDS grants R01 NS062822 and R01 NS097550 to J.S.D.

Received: June 4, 2017
Revised: August 14, 2017
Accepted: October 1, 2017
Published: October 24, 2017

REFERENCES

Arber, S. (2012). Motor circuits in action: specification, connectivity, and function. Neuron *74*, 975–989.

Catela, C., Shin, M.M., and Dasen, J.S. (2015). Assembly and function of spinal circuits for motor control. Annu. Rev. Cell Dev. Biol. *31*, 669–698.

Chen, J.A., Huang, Y.P., Mazzoni, E.O., Tan, G.C., Zavadil, J., and Wichterle, H. (2011). Mir-17-3p controls spinal neural progenitor patterning by regulating Olig2/Irx3 cross-repressive loop. Neuron *69*, 721–735.

Dasen, J.S. (2017). Master or servant? Emerging roles for motor neuron subtypes in the construction and evolution of locomotor circuits. Curr. Opin. Neurobiol. *42*, 25–32.

Dasen, J.S., Tice, B.C., Brenner-Morton, S., and Jessell, T.M. (2005). A Hox regulatory network establishes motor neuron pool identity and target-muscle connectivity. Cell *123*, 477–491.

Dasen, J.S., De Camilli, A., Wang, B., Tucker, P.W., and Jessell, T.M. (2008). Hox repertoires for motor neuron diversity and connectivity gated by a single accessory factor, FoxP1. Cell *134*, 304–316.

Dessaud, E., Yang, L.L., Hill, K., Cox, B., Ulloa, F., Ribeiro, A., Mynett, A., Novitch, B.G., and Briscoe, J. (2007). Interpretation of the sonic hedgehog morphogen gradient by a temporal adaptation mechanism. Nature *450*, 717–720.

Eccles, J.C., Eccles, R.M., and Lundberg, A. (1957). The convergence of monosynaptic excitatory afferents on to many different species of alpha motoneurones. J. Physiol. *137*, 22–50.

Eide, A.L., and Glover, J.C. (1995). Development of the longitudinal projection patterns of lumbar primary sensory afferents in the chicken embryo. J. Comp. Neurol. *353*, 247–259.

Frank, E., and Mendelson, B. (1990). Specification of synaptic connections between sensory and motor neurons in the developing spinal cord. J. Neurobiol. *21*, 33–50.

Goetz, C., Pivetta, C., and Arber, S. (2015). Distinct limb and trunk premotor circuits establish laterality in the spinal cord. Neuron *85*, 131–144.

Goulding, M. (2009). Circuits controlling vertebrate locomotion: moving in a new direction. Nat. Rev. Neurosci. *10*, 507–518.

Grillner, S. (2006). Biological pattern generation: the cellular and computational logic of networks in motion. Neuron *52*, 751–766.

Hinckley, C.A., Alaynick, W.A., Gallarda, B.W., Hayashi, M., Hilde, K.L., Driscoll, S.P., Dekker, J.D., Tucker, H.O., Sharpee, T.O., and Pfaff, S.L. (2015). Spinal locomotor circuits develop using hierarchical rules based on motorneuron position and identity. Neuron *87*, 1008–1021.

Jessell, T.M., Sürmeli, G., and Kelly, J.S. (2011). Motor neurons and the sense of place. Neuron *72*, 419–424.

Jung, H., Lacombe, J., Mazzoni, E.O., Liem, K.F., Jr., Grinstein, J., Mahony, S., Mukhopadhyay, D., Gifford, D.K., Young, R.A., Anderson, K.V., et al. (2010). Global control of motor neuron topography mediated by the repressive actions of a single hox gene. Neuron *67*, 781–796.

Livet, J., Sigrist, M., Stroebel, S., De Paola, V., Price, S.R., Henderson, C.E., Jessell, T.M., and Arber, S. (2002). ETS gene *Pea3* controls the central position and terminal arborization of specific motor neuron pools. Neuron *35*, 877–892.

Luo, L., and O'Leary, D.D.M. (2005). Axon retraction and degeneration in development and disease. Annu. Rev. Neurosci. *28*, 127–156.

Machado, T.A., Pnevmatikakis, E., Paninski, L., Jessell, T.M., and Miri, A. (2015). Primacy of flexor locomotor pattern revealed by ancestral reversion of motor neuron identity. Cell *162*, 338–350.

Mendell, L.M., and Henneman, E. (1968). Terminals of single Ia fibers: distribution within a pool of 300 homonymous motor neurons. Science *160*, 96–98.

Mendelsohn, A.I., Simon, C.M., Abbott, L.F., Mentis, G.Z., and Jessell, T.M. (2015). Activity regulates the incidence of heteronymous sensory-motor connections. Neuron *87*, 111–123.

Ozaki, S., and Snider, W.D. (1997). Initial trajectories of sensory axons toward laminar targets in the developing mouse spinal cord. J. Comp. Neurol. *380*, 215–229.

Pecho-Vrieseling, E., Sigrist, M., Yoshida, Y., Jessell, T.M., and Arber, S. (2009). Specificity of sensory-motor connections encoded by Sema3e-Plxnd1 recognition. Nature *459*, 842–846.

Philippidou, P., and Dasen, J.S. (2013). Hox genes: choreographers in neural development, architects of circuit organization. Neuron *80*, 12–34.

Rossignol, S., Dubuc, R., and Gossard, J.P. (2006). Dynamic sensorimotor interactions in locomotion. Physiol. Rev. *86*, 89–154.

Rousso, D.L., Gaber, Z.B., Wellik, D., Morrisey, E.E., and Novitch, B.G. (2008). Coordinated actions of the forkhead protein Foxp1 and Hox proteins in the columnar organization of spinal motor neurons. Neuron *59*, 226–240.

Song, J., Ampatzis, K., Björnfors, E.R., and El Manira, A. (2016). Motor neurons control locomotor circuit function retrogradely via gap junctions. Nature *529*, 399–402.

Stepien, A.E., Tripodi, M., and Arber, S. (2010). Monosynaptic rabies virus reveals premotor network organization and synaptic specificity of cholinergic partition cells. Neuron *68*, 456–472.

Sürmeli, G., Akay, T., Ippolito, G.C., Tucker, P.W., and Jessell, T.M. (2011). Patterns of spinal sensory-motor connectivity prescribed by a dorsoventral positional template. Cell *147*, 653–665.

Tripodi, M., Stepien, A.E., and Arber, S. (2011). Motor antagonism exposed by spatial segregation and timing of neurogenesis. Nature *479*, 61–66.

Vrieseling, E., and Arber, S. (2006). Target-induced transcriptional control of dendritic patterning and connectivity in motor neurons by the ETS gene *Pea3*. Cell *127*, 1439–1452.